universe

MDPI

Communication

Peculiarities of the Heliospheric State and the Solar-Wind/Magnetosphere Coupling in the Era of Weakened Solar Activity

Yuri I. Yermolaev *, Irina G. Lodkina, Alexander A. Khokhlachev and Michael Yu. Yermolaev

Space Research Institute, Russian Academy of Sciences, 117997 Moscow, Russia
* Correspondence: yermol@iki.rssi.ru

Abstract: Based on the data of the solar wind (SW) measurements of the OMNI database for the period 1976–2019, we investigate the behavior of SW types, as well as plasma and interplanetary magnetic field (IMF) parameters, for 21–24 solar cycles (SCs). Our analysis shows that with the beginning of the period of low solar activity (SC 23), the number of all types of disturbed events in the interplanetary medium decreased, but the proportion of magnetic storms initiated by CIR increased. In addition, a change in the nature of SW interaction with the magnetosphere could occur due to a decrease in the density, temperature, and IMF of solar wind.

Keywords: solar wind; magnetosphere; geomagnetic activity; magnetic storm; space weather

Citation: Yermolaev, Y.I.; Lodkina, I.G.; Khokhlachev, A.A.; Yermolaev, M.Y. Peculiarities of the Heliospheric State and the Solar-Wind/Magnetosphere Coupling in the Era of Weakened Solar Activity. *Universe* **2022**, *8*, 495. https://doi.org/10.3390/universe8100495

Academic Editor: Luca Sorriso-Valvo

Received: 14 August 2022
Accepted: 20 September 2022
Published: 22 September 2022

1. Introduction

The state of the magnetosphere is determined by two competing processes: excitation by external, interplanetary drivers and relaxation due to internal, magnetospheric and ionospheric processes. The following disturbed phenomena of solar wind (SW) are considered as the main interplanetary drivers, which may contain the southward component of the interplanetary magnetic field (IMF) and be geoeffective: interplanetary coronal mass ejections (ICMEs; in this paper, we consider two subtypes of ICMEs, magnetic clouds and ejecta, together), compression areas before ICMEs, sheaths, and compression areas between fast and slow SW streams, corotating interaction regions (CIRs) [1–5].

Solar scientists have long drawn attention to a noticeable decrease in solar activity [6,7], but solar wind and magnetosphere specialists relatively rarely pay attention to this fact (for example, [8,9]) and usually do not take into account the possible change in the properties of SW and interplanetary drivers during the space era. Recently, on the basis of data from the OMNI database for solar cycles (SCs) 21–24, we showed [10] that in the interval between solar cycles 22 and 23, the structure of the heliosphere changed, and most of the SW and IMF parameters were reduced by 20–40%; this drop was observed in all types of SW and all phases of SCs. These changes in SW could lead to changes in solar-wind/magnetosphere coupling, in particular, to a sharp decrease in the number of magnetic storms in SCs 23 and 24. In this short paper, we consider some experimental data on SW and the magnetosphere related to the long-term, on the scale of four solar cycles, weakening of the SW and its effect on solar–terrestrial links.

2. Data and Methods

In this work, we use two sources of information for 1976–2019: (1) hourly data of solar wind measurements and magnetospheric indices in the OMNI database (https://spdf.gsfc.nasa.gov/pub/data/omni/low_res_omni, [11] (accessed on 1 February 2022)) and (2) intervals of different types of SW in the catalog of large-scale phenomena (http://www.iki.rssi.ru/pub/omni, [12] (accessed on 1 February 2022)) created on the basis of the OMNI database. The procedure for identifying solar wind types based on a set of

threshold criteria for key parameters is described in detail in [12]. To present data on the distribution of solar wind types (bottom panels of Figures 1 and 2) and on the distribution of magnetic storms induced by different types of interplanetary drivers (upper panel of Figure 2), we use the parameters of fraction of SW events and fraction of storms. The fraction of events refers to the ratio of the total time of registration of the selected type of SW to the total time of measurement of all types of SW in the interval under study (for example, [13]). The fraction of storms refers to the ratio of the total observation time of a magnetic storm induced by a given SW type to the duration of all magnetic storms over the studied time interval.

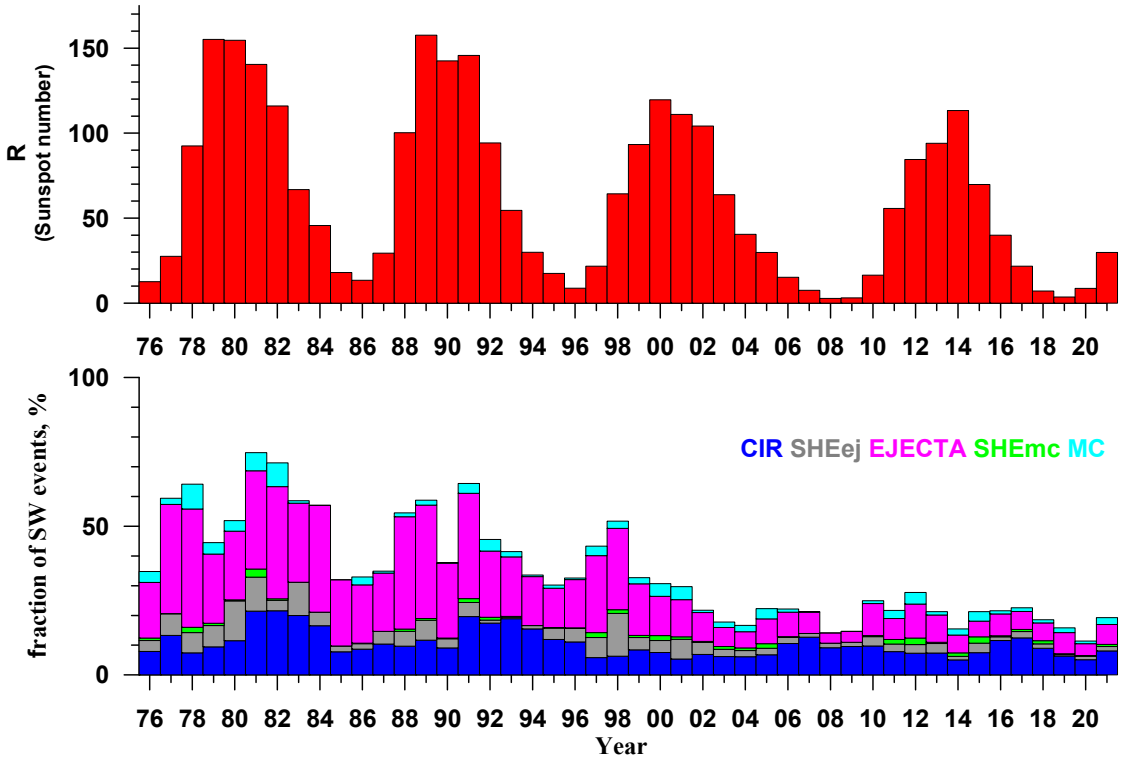

Figure 1. Yearly number of sunspots (upper panel) and fractions of disturbed SW events (bottom panel; legend is shown on the panel) during the period of 1976–2021.

Due to the relatively small number of magnetic clouds, we analyzed them together with ejecta as a general class of ICME drivers and did not separate sheath compression areas before MC and ejecta. The parameters of solar wind are highly variable, and when calculating the average parameters, relatively large standard deviations were obtained. However, given that a large number of measurement points (up to several thousand) were used, statistical errors (standard deviations divided by the square root of the number of points) were small, and the obtained average values of the parameters have a high degree of statistical significance [10,14]. In particular, the statistical errors do not exceed the size of the symbols in the figures below.

To determine magnetic storms, a standard criterion is used: the minimum Dst index is less than −50 nT [1,2]. When associating interplanetary and magnetospheric phenomena, it was assumed that the magnetic storm was generated by the type of interplanetary driver within which the minimum of Dst index fell.

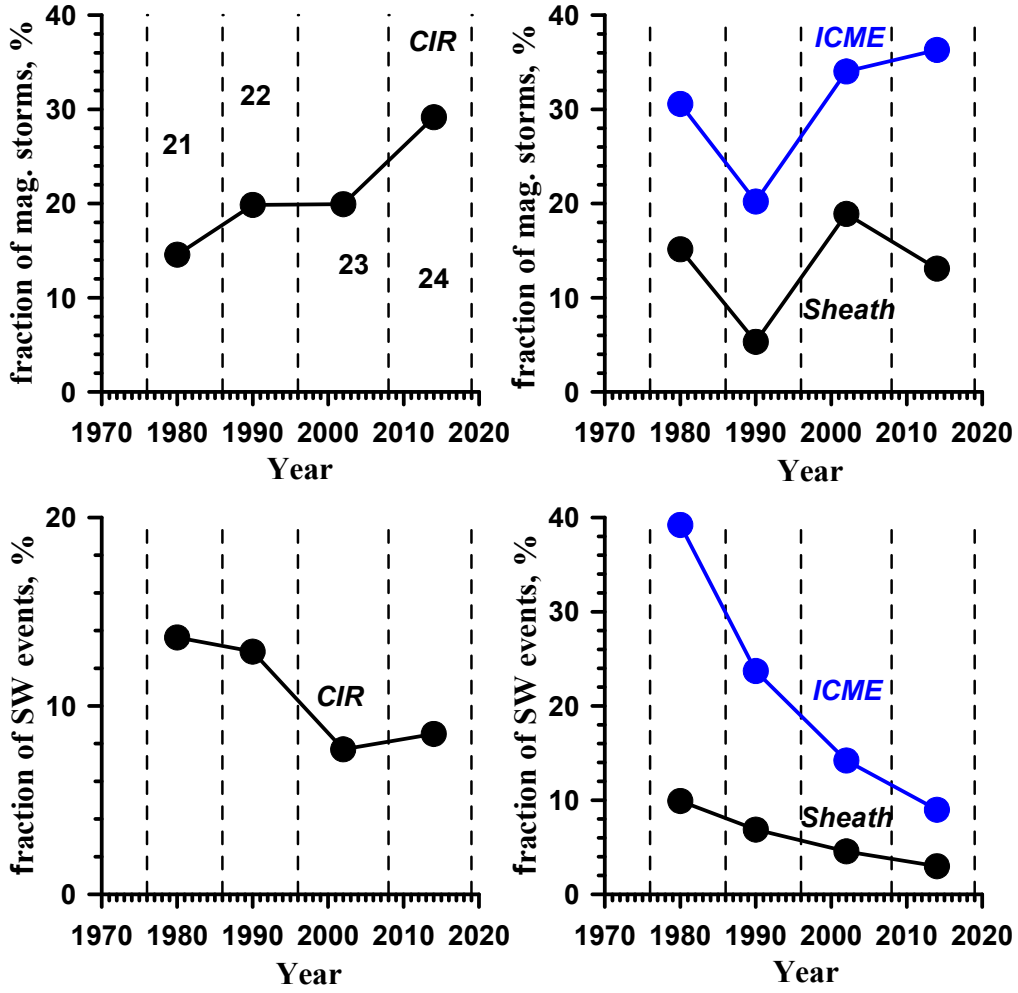

Figure 2. Temporal profiles of fraction of magnetic storms (upper panels) and fraction of SW events (bottom panels) during solar cycles 21–24: for CIRs (left panels), sheaths (right panels, black circles) and ICMEs (right panels, blue circles).

3. Results and Discussion

Recently, we showed [10] that in SCs 23 and 24, the number of ICMEs and sheaths dropped significantly, whereas the number and distribution of CIRs did not change significantly. This can be illustrated by the data for 1976–2021 shown in Figure 1. The upper panel of the figure shows the annual number of sunspot, and the filled columns in the lower panel represent the annual fraction of disturbed solar wind types (the legend is shown in the figure): MC, sheaths in front of MC, SHEmc, ejecta, sheaths in front of ejecta, SHEej, and CIR. The unshaded parts of the columns correspond to quasi-stationary types of SW: fast and slow SW flows and the heliospheric current sheet (HCS). In general, the temporal behavior of the disturbed SW types in solar cycles repeats the previously discovered patterns (for example, [13]): the increase in the number of CME-related events near SC maxima and the increase in the number of CIR events near the SC decline and minimum phases. However, the reduction in the number of perturbed SW types occurred during total period covering SCs 21–24 and not only at the end of the 20th century (at the beginning of SC 23), when a reduction in SW parameters was observed [10].

Because the task of this work is to study long-term variations, Figure 2 shows the temporal behavior of parameters averaged over solar cycles. For this figure, we combined the intervals SHEmc and SHEej into a common sheath type and MC and ejecta into an ICME type. Data in the bottom panels of Figure 2 show the fraction of the total observation time during which different disturbed SW types are observed: CIR (left panel) and ICME and sheath (right panel). The CIR time share decreased slightly from ~13 to ~9%, whereas the

ICME and sheath time shares fell from ~40 to ~8% and ~10 to ~3%, respectively. The total number of disturbed SW types fell from ~60 to ~20%. An interesting feature is observed: if the ICME and sheath time fractions exhibit a common global decreasing trend over the total period covering SCs 21–24, the CIR time fraction significantly decreases in the SC 22–23 interval, and this interval coincides with the beginning of the decline in the SW and IMF parameters [10]. The data in the top two panels of Figure 2 show the proportion of medium and strong magnetic storms (Dst < −50 nT) generated by CIR (left panel) and ICME and sheath (right panel) events. These panels show that against the background of a general decrease in the number of magnetic storms (for example, Figure 2 in [10]), the proportion of storms generated by ICMEs and sheaths behave nonmonotonically; for ICMEs, the proportion exhibits a general upward trend from ~30% in SC 21 to ~38% in SC 24 but with a noticeable decrease to ~20% in SC 22. For sheaths, the proportion is ~14% in SC 21 and SC 24 but decreases to ~6% in SC 22 and increases to ~19% in SC 23, whereas the proportion of CIR-induced storms markedly increases from ~17 to ~30%.

The fact noted above that the number of storms does not change easily in proportion to the number of corresponding SW drivers can be associated with changes in the parameter values of the SW and IMF during SCs 21–24. Figure 3 presents the cycle average values of the density, velocity, IMF magnitude, and solar wind proton temperature for four SCs. Only the speed remains approximately unchanged (within 10%); the other three parameters are significantly reduced. How these (and some other) parameters decrease during certain phases of solar cycles and in certain types of SW, including the main interplanetary drivers of magnetospheric disturbances, can is shown in corresponding figures in [10]. A comparison of the detailed time profiles of 21 solar wind parameters and magnetospheric indices in disturbed SW types during the epochs of high and low solar activity is presented in [14]. Here, we want to note only some important general facts.

(1) Because during SCs 23–24, the temperature and IMF value dropped at a constant velocity, the sonic and Alfvén Mach numbers in the solar wind increased, i.e., in the present epoch, the magnetosphere is flowed around by more "supersonic" and more "super-alfvenic" SW than in the previous SCs 21–22. In addition, the drop in the beta parameter (not shown here but presented in [10]) indicates that the drop in magnetic pressure was less than the drop in thermal pressure. Therefore, the regime of the SW flow around the magnetosphere of the Earth and their interaction may differ from that during the previous period.

(2) Because the density and dynamic pressure dropped by ~30% during SCs 23–24, the pressure balance of the interplanetary plasma and the magnetospheric plasma at the magnetopause was located further from the center of the Earth, i.e., the size of the magnetosphere and its structures has increased, and the pressure inside the magnetosphere decreased. This can affect both the nature of SW interaction with the magnetosphere and the physical processes within the magnetosphere [8,15,16].

(3) For the epoch of high solar activity, it was shown that the efficiency of excitation of magnetic storms is higher for sheath and CIR events than for ICMEs [3,13]. The relative number of disturbed SW streams, especially those associated with CME, dropped significantly during the epoch of low solar activity. In [10,14], we noted a drop in the main parameters of plasma and IMF in all types of SW, and in the disturbed types, the reduction in parameters was greater than in the undisturbed types. Differences in the reduction in different parameters in different interplanetary drivers can affect the efficiency of different types of SW.

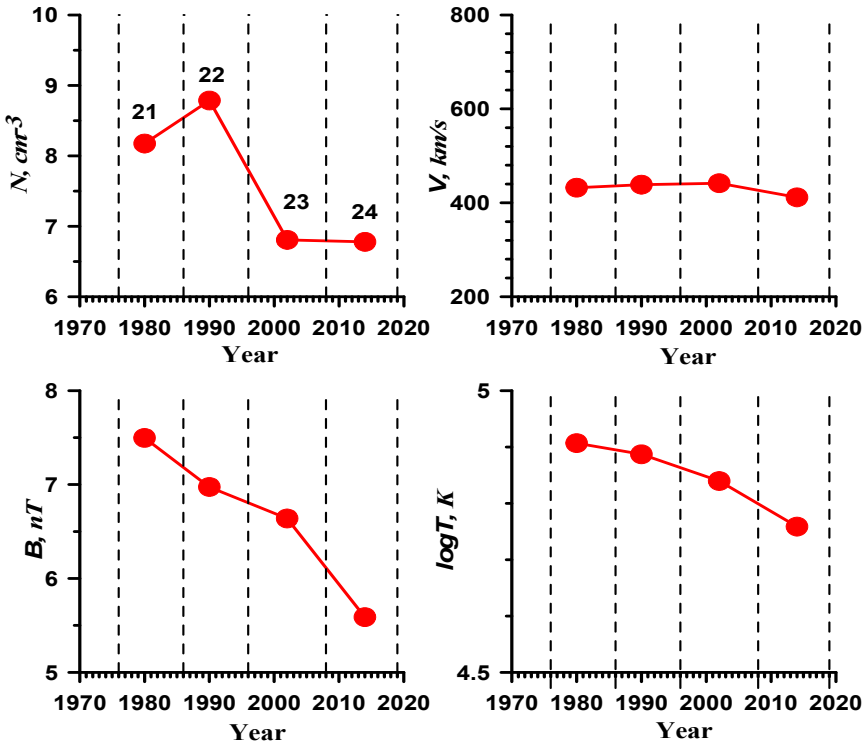

Figure 3. Temporal profiles of yearly averaged density (N), velocity (V), magnitude IMF (B) and proton temperature (T) during solar cycles 21–24.

Because for all the data presented with respect to the identification of SW types, a standard technique was used in which key parameters are compared with constant threshold conditions, it cannot be ruled out that some disturbed SW types cannot be identified by standard techniques with decreasing parameter values. However, the question of creating new system thresholds for the classification of SW phenomena for the epoch of low solar activity requires additional research and consensus among the scientific community.

4. Conclusions

An analysis of measurements of solar wind parameters during the period of 1976–2019 showed that the fall in solar activity during SCs 23–24 was accompanied by a weakening of the characteristics and a change in the structure of the interplanetary medium. This, in particular, is accompanied by a decrease in the number of all types of disturbed events in the interplanetary medium and an increase in the relative contribution of CIR compression regions to the excitation of magnetic storms against the background of a decrease in the number of ICMEs and sheath events. In addition, the SW density, temperature, and IMF decrease significantly, which can lead to a change in the nature of the solar wind flow around the magnetosphere and their interaction. Therefore, the data on direct measurements of solar-wind/magnetosphere coupling obtained during the space era may differ for physical reasons, analysis thereof must be divided into the initial period of the space era and the period of low solar activity. It is also important to account for changes in numbers and properties of external drivers to predict space weather effects.

Author Contributions: Conceptualization, Y.I.Y.; methodology, Y.I.Y.; software, I.G.L. and A.A.K.; validation, M.Y.Y., data curation, I.G.L.; writing—original draft preparation, Y.I.Y.; writing—review and editing, Y.I.Y.; visualization, I.G.L.; supervision, Y.I.Y. All authors have read and agreed to the published version of the manuscript.

Funding: The work was supported by the Russian Science Foundation, grant 22-12-00227.

Acknowledgments: The authors thank the creators of the OMNI databases, which were used in this work (https://spdf.gsfc.nasa.gov/pub/data/omni/low_res_omni accessed on 1 February 2022; http://www.iki.rssi.ru/pub/omni; accessed on 1 February 2022).

Conflicts of Interest: The authors declare no conflict of interest.

References

1. Gonzalez, W.D.; Tsurutani, B.T.; Clua de Gonzalez, A.L. Interplanetary origin of geomagnetic storms. *Space Sci. Rev.* **1999**, *88*, 529–562. [CrossRef]
2. Yermolaev, Y.I.; Yermolaev, M.Y.; Zastenker, G.N.; Zelenyi, L.M.; Petrukovich, A.A.; Sauvaud, J.A. Statistical studies of geomagnetic storm dependencies on solar and interplanetary events: A review. *Planet. Space Sci.* **2005**, *53*, 189–196. [CrossRef]
3. Yermolaev, Y.I.; Lodkina, I.G.; Dremukhina, L.A.; Yermolaev, M.Y.; Khokhlachev, A.A. What solar–terrestrial link researchers should know about interplanetary drivers. *Universe* **2021**, *7*, 138. [CrossRef]
4. Borovsky, J.E.; Denton, M.H. Differences between CME-driven storms and CIR-driven storms. *J. Geophys. Res.* **2006**, *111*, A07S08. [CrossRef]
5. Kilpua, E.K.J.; Fontaine, D.; Moissard, C.; Ala-Lahti, M.; Palmerio, E.; Yordanova, E.; Turc, L. Solar wind properties and geospace impact of coronal mass ejection-driven sheath regions: Variation and driver dependence. *Space Weather.* **2019**, *17*, 1257–1280. [CrossRef]
6. Feynman, J.; Ruzmaikin, A. The Sun's strange behavior: Maunder minimum or Gleissberg cycle? *Sol. Phys.* **2011**, *272*, 351–363. [CrossRef]
7. Zolotova, N.V.; Ponyavin, D.I. Is the new Grand minimum in progress? *J. Geophys. Res. Space Phys.* **2014**, *119*, 3281–3285. [CrossRef]
8. Oh, S.; Kim, B. Variation of solar, interplanetary and geomagnetic parameters during solar cycles 21-24. *J. Astron. Space Sci.* **2013**, *30*, 101–106. [CrossRef]
9. Gopalswamy, N.; Yashiro, S.; Xie, H.; Akiyama, S.; Makela, P. Properties and geoeffectiveness of magnetic clouds during solar cycles 23 and 24. *J. Geophys. Res. Space Phys.* **2015**, *120*, 9221–9245. [CrossRef]
10. Yermolaev, Y.I.; Lodkina, I.G.; Khokhlachev, A.A.; Yermolaev, M.Y.; Riazantseva, M.O.; Rakhmanova, L.S.; Moskaleva, A.V. Drop of solar wind at the end of the 20th century. *J. Geophys. Res. Space Phys.* **2021**, *126*, e2021JA029618. [CrossRef]
11. King, J.H.; Papitashvili, N.E. Solar wind spatial scales in and comparisons of hourly wind and ACE plasma and magnetic field data. *J. Geophys. Res.* **2005**, *110*, A02209. [CrossRef]
12. Yermolaev Yu, I.; Nikolaeva, N.S.; Lodkina, I.G.; Yermolaev, M.Y. Catalog of Large-Scale Solar Wind Phenomena during 1976-2000. *Cosm. Res.* **2009**, *47*, 81–94. [CrossRef]
13. Yermolaev, Y.I.; Nikolaeva, N.S.; Lodkina, I.G.; Yermolaev, M.Y. Geoeffectiveness and efficiency of CIR, sheath, and ICME in generation of magnetic storms. *J. Geophys. Res.* **2012**, *117*, A00L07. [CrossRef]
14. Yermolaev, Y.I.; Lodkina, I.G.; Khokhlachev, A.A.; Yermolaev, M.Y.; Riazantseva, M.O.; Rakhmanova, L.S.; Borodkova, N.L.; Sapunova, O.V.; Moskaleva, A.V. Dynamics of Large-Scale Solar-Wind Streams Obtained by the Double Superposed Epoch Analysis: 5. Influence of the Solar Activity Decrease. *Universe* **2022**, *8*, 472. [CrossRef]
15. Antonova, E.E.; Kirpichev, I.P.; Stepanova, M.V. Plasma pressure distribution in the surrounding the Earth plasma ring and its role in the magnetospheric dynamics. *J. Atmos. Sol. Terr. Phys.* **2014**, *115*, 32. [CrossRef]
16. Kirpichev, I.P.; Antonova, E.E.; Stepanova, M. Ion leakage at dayside magnetopause in case of high and low magnetic shears. *J. Geophys. Res. Space Phys.* **2017**, *122*, 8078–8095. [CrossRef]